**Journal of Engineering and Sustainable Development**
Vol. 30, No. 04, July 2026
https://jeasd.uomustansiriyah.edu.iq/index.php/jeasd
ISSN 2520-0917
**Research Article**
https://doi.org/10.31272/jeasd.2100

# Structural Behavior of Composite Beam Subjected to Impact Loading

Ayad Hasan Jawad*, Hesham A. Numan

Civil Engineering Department, College of Engineering, Mustansiriyah University, Baghdad.

*Email: ayaidhasan@uomustansiriyah.edu.iq

**Article Info**

| | |
|---|---|
| **Received** | **25/07/2024** |
| **Revised** | **07/05/2026** |
| **Accepted** | **15/05/2026** |

**Abstract**

Composite beams are widely used members in different applications and are subjected to various loads. Impact load is one of the dynamic loads generated by falling objects striking structural members, producing a short-duration load. This load affects the member's structural performance, reducing it. In this study, a composite beam with a pultruded I-section was numerically investigated using finite element software. The model was validated by a previous experimental model conducted by a previous researcher. The model consists of a pultruded I-section and 20 MPa concrete slabs; the parameters studied here are three concrete compressive strengths: 50, 75, and 100 MPa. Alternative reinforcement types to steel bars, such as Glass Fiber Reinforced Polymer (GFRP) and Carbon Fiber Reinforced Polymer (CFRP) bars, were also studied. It was found that increasing concrete compressive strength decreases the impact effect on the composite beam. When Glass Fiber Reinforced Polymer bars were used, the stiffness of the impacted beam was reduced by 40% and ductility by 25%, making them the most vulnerable bars under impact.

**Keywords:** Carbon Fiber Reinforced Polymer Bars, Composite Beam, Glass Fiber Reinforced Polymer Bars, Impact Load.

## 1. Introduction

Composite members are widely used in various bridges and buildings. They utilize the best characteristics of steel and concrete. As is known, concrete is quite good at compression, but it's weak in tension, so steel is used to solve this defect. This makes steel-concrete composite constructions highly effective and cost-saving compared to other alternatives considered for the same load magnitudes or functions. The steel-concrete composite beam is one of the earliest composite constructions used [1]-[4]. Several composite beams are shown earlier. The first patent for stone composite beams was obtained by Ralph Dodd in 1808, and the technology then evolved to incorporate iron, concrete, and other developments up to 1975, when the composite beam began to be used in its popular shape [5], [6]. Composite constructions offer many advantages, making them the best option for many designs. They tend to have greater stiffness, load, and collapse capacities, which lead to smaller sections and reduced material usage [2]–[7]. Due to the continuous need for materials and cost savings, or to provide desired properties, various constituents were used instead of steel, such as Fiber-Reinforced Polymer (FRP) and even wood, as shown in Fig. 1 [8], but steel-concrete sections are the most common [9]-[12].

These components are assembled with shear connectors to ensure they are used compositely and function as a single unit [13]. This composite action increases the load-carrying capacity and stiffness of the composite beam by a factor of 2 to 3.5 [14]. Various types of loads may be applied to these structures, such as monotonic, dynamic, and impact loads. The main difference between monotonic load and impact load is the short duration of the impact [15]. Composite beams are more vulnerable to impact damage because they cause the interior to degrade, which may not be easily visible and may reduce the performance of the structure [16], so impact events should be taken into consideration in the design of these members or structures. This paper numerically investigates the behavior of composite beams under monotonic and impact loading, using experimental data reported in the literature.

## 2. Background

Many researchers investigated the behavior of composite beams under different load circumstances and various types of shear connectors in monotonic field tests. The behavior of composite beams under sustained loads over a long period (3 years) is studied by Fan et al. [17]. A set of beams under negative and positive bending moments was examined. The finding of this study was that under the effect of a positive bending moment, the deflection was 2.5 times the initial deflection, and concrete

cracking occurred due to combined shrinkage and a negative moment. Machado et al [18] developed numerical dynamic analysis for composite beams. Partial interconnection was taken into account. The analysis involves determining the natural frequencies and mode shapes by varying the stiffness of the connection. It was concluded that as stiffness decreased, a higher-order mode shape appeared. After performing a numerical investigation to obtain the failure process of the composite beam, a conclusion obtained by Zhao and Li [19] that the composite beam has three major failure modes can be summarized as follows: "cracking of the concrete by the local tensile stress, crushing of the concrete by the compressive stress, and extensive yielding of the steel beam under the global bending moment".

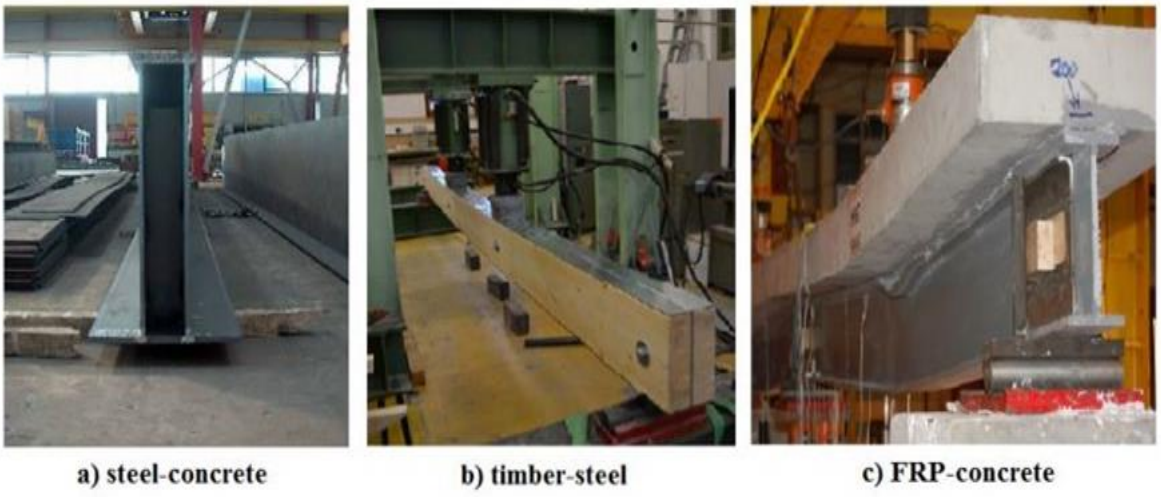


**Figure 1.** Different types of composite beams [8].

The effect of using high-strength steel on the behavior of composite beams is studied by Shamass and Cashell [20]. Two grades of steel were used (S690 and S460). It has been found that the slip is greater for beams with S690. This is because increased yield strength results in greater load capacity and a larger relative displacement between the two materials. In a dynamic field investigation, the behavior of composite beams under impact loads was experimentally studied by Xiao et al. [21]. The sand layer was used as an energy dissipater. The experimental test was accompanied by elastic-plastic analysis. The authors declared that the main failure mode was longitudinal splitting of the concrete, with an error between test and analysis results of less than 15.82%. The effect of harmonic force and static load on a partially interconnected composite beam was investigated by Hamood et al. [22]; they disclosed that the static load had the largest effect on mid-span deflection and slip, while the dynamic influence was related to the load amplitude. Some researchers [23]–[26] investigated the response of composite beams under different applied loading systems, including shear loading, monotonic loading, vertical point loading, and dynamic cycling loading. All the tests proved the reliability of composite beams for different applications. Other materials were investigated by researchers such as Neagoe et al [27], who studied the pultruded Glass Fiber Reinforced Polymer (GFRP) composite beam. The study found that the GFRP composite beam is structurally sound and efficient, with a high flexural capacity-to-self-weight ratio, and exhibits 50% higher ultimate capacity and lower weight than reinforced concrete. Allawi and Ali [28] investigated the composite beam under the effect of impact load. Two compressive strengths of concrete were used (20 and 50 MPa. They reported that the 50 MPa slab has a higher deflection than the 20 MPa slab, and that the damping time of high-strength concrete specimens subjected to impact loading is 59% longer than that of the normal-strength concrete specimen. This study investigates the effects of impact on a composite beam, examines how increased concrete strength could help the beam resist impact, and explores the possibility of using CFRP and GFRP bars under such circumstances.

## 3. Methods and Materials

### 3.1 Specimen Description

An experimental work reported by Allawi and Ali [28] was used to validate the finite element model. The test was performed on a pultruded Glass Fiber Reinforced Polymer (GFRP)-concrete composite beam and focused on impact loading. The specimen consists of a concrete slab 500mm wide, 80mm thick, and 3000mm long, with a compressive strength of 20 MPa. Reinforced by 6 mm bars spaced at 75 mm. A pultruded GFRP I-section with a width of 100mm, a thickness of 10mm for both the top and bottom flanges, and a total depth of 150 mm, linked to the concrete slab by an inverted U-hook shear connector with a diameter of 12mm at 300 mm, as shown in Fig. 2 they would be referred to as the reference specimen. Details of the experiment, including geometry, loading, boundary conditions, and material properties, are presented. The effects of concrete compressive strength and bar type on the behavior of composite beams were investigated. Concrete compressive strengths of 50, 75, and 100 MPa were used, and in addition to the steel bars, Glass Fiber Reinforced Polymer (GFRP) and Carbon Fiber Reinforced Polymer (CFRP) bars

were used. The GFRP bars have a tensile strength of 503 MPa and modulus of elasticity of 25.6 GPa [29], while CFRP bars have a tensile strength of 2068MPa and modulus of elasticity of 124 GPa [30]. The reference specimen consists of a GFRP section and a 20 MPa concrete slab reinforced with 6 mm steel bars.

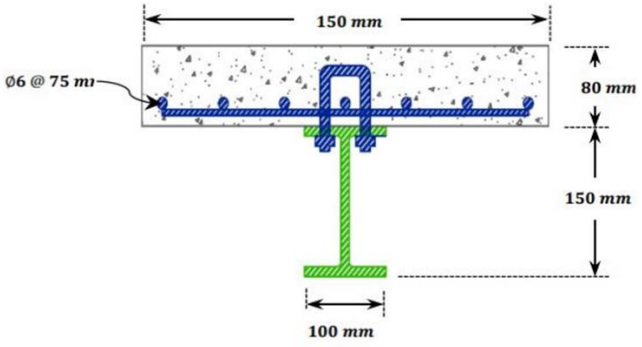


**Figure 2.** Composite beam cross-section [28]

### 3.2. Numerical Modeling

Among the various techniques available to engineers, Finite Element Analysis (FEA) is one of the most diverse ones to use. Numerical methods are the most powerful analytical approaches in engineering for dealing with complex geometries. In the present work, three-dimensional modeling for composite GFRP-concrete beams was evaluated under impact load. The finite element analysis using the (ABAQUS 2020) program included real-time experimental simulation on beams to be investigated, as shown in Fig. 3. The composite beams and deck slab were modeled using 3D stress elements, and the GFRP was modeled using 3D shell elements. The reinforcement steel and shear connectors were modeled using ordinary 2D elements. An eight-node solid brick element (C3D8R) with 8 node integration points was used to represent the concrete volume. Longitudinal and transverse steel bars were modeled utilizing an embedded truss reinforcement of a 2-node linear truss element (T3D2). Steel plates under applied loads and resistive reactions were also modeled using eight-node solid components. A 4-node 3-D bilinear rigid quadrilateral (R3D4) was used to model the impactor. It is worth noting that the perfect bond between the surrounding concrete and the steel bars was assumed in this analysis. The FRP composite material model (Hashin damage model) was used to model the pultruded profiles with a Linear quadrilateral, type S4R element. For the concrete analysis, the damaged plasticity model (DPM) was applied. This model describes the irreversible damage that occurs during fracturing by combining non-associated multi-hardening plasticity and scalar (isotropic) elasticity. This model's primary failure mechanisms are tensile cracking and compressive crushing of concrete [31].

For the meshing process, an approximate global size of 30 was used as shown in Fig. 4 with a total number of elements of 15071 detailed as follows, 1340 linear quadrilateral elements of type S4R for the GFRP section, 12660 linear hexahedral elements of type C3D8R for the concrete slab, 723 linear line elements of type T3D2 for the reinforcements, and 384 Linear quadrilaterals element type R3D4 for the impactor in addition to a Total number of nodes of 20280.

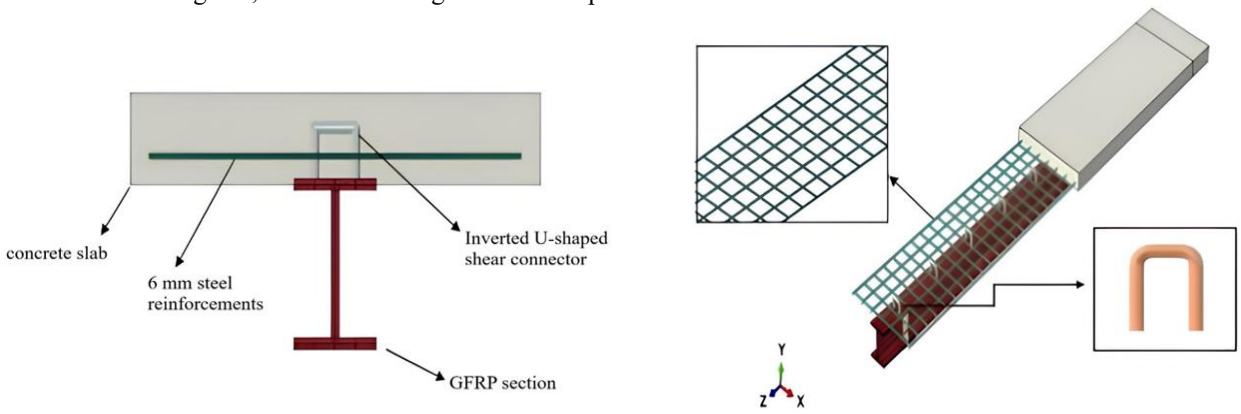


**Figure 3.** ABAQUS-constructed specimen details.

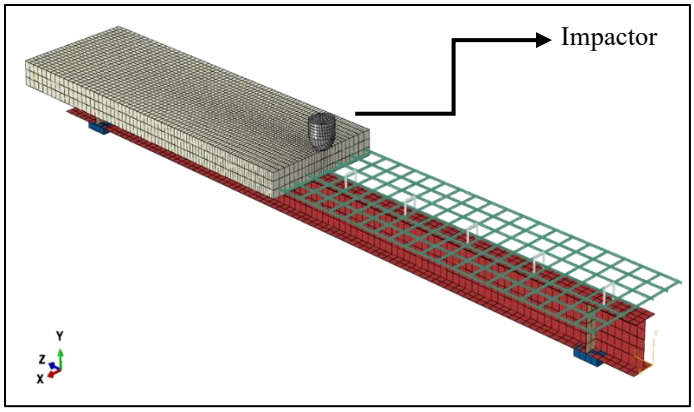


**Figure 4.** The meshing of the simulated model.

### 3.3. Loading Process and Data Comparison

The simulated specimens were tested in two groups, each comprising five beams (three composite beams with different concrete compressive strengths and two beams reinforced with GFRP and CFRP bars), compared with the reference beam, which had a 20 MPa concrete slab reinforced with steel bars. The first group was tested under a pure monotonic load until failure. Each beam in the second group was analyzed under the effect of an impact load from a 25kg mass falling freely from a height of 2m, at a speed calculated using the equation of velocity equal to the square root [32], and then subjected to incremental monotonic loading up to failure, as clarified in Fig.5.

$$V=\sqrt{2\,g\,h} \quad (1)$$

Were

V = the impactor velocity

g = the acceleration

h = the impactor high

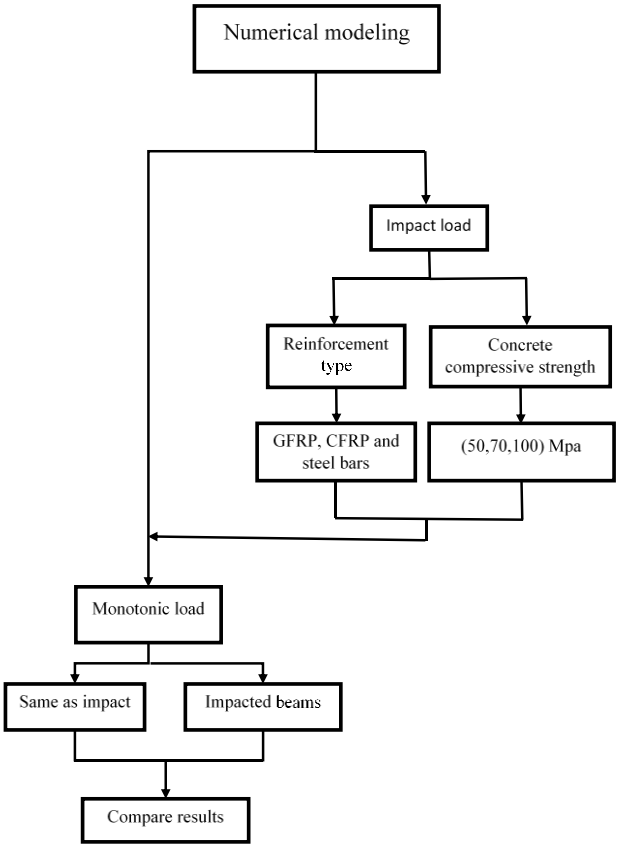


**Figure 5.** Loading process.

The experimental impact force was 46.5 kN, while the numerical force was 42 kN. Figs. 6 and 7 clarify the experimental and numerical behavior under both monotonic and impact loads, and the differences between them, for the pure monotonic load. The maximum experimental load was 122.34 kN, while the numerical maximum load was 116.51 kN; the maximum percentage error was 5% for the specimens tested under the effect of monotonic loads, while the percentage error for the impacted beams was 6.5%. The maximum experimental load was 95.85 kN, while the numerical maximum load was 90 kN.

## 4. Results and Discussion

The specimen could support a maximum monotonic load of 116.51 kN before the impact load application, which caused the load to drop to 90 kN, indicating a 22.66% reduction in load-carrying capacity, as shown in Fig. 8.

The failure mode was transformed before and after the collision, as seen in Figs. 9 and 10. As shown in the application of pure monotonic load, the fractures in the slab extend virtually down the slab and in areas surrounding the connectors. The cracks formed around the impacted area because the impact force of the falling mass weakened the area.

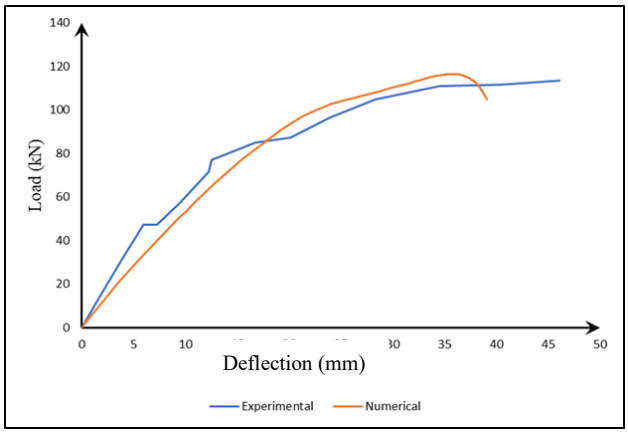


**Figure 6.** Data comparison for beams under monotonic load.

### 4.1. Effect of Concrete Compressive Strength

*4.1.1. Failure mode and load-displacement behavior*

When a concrete compressive strength of 50 MPa was used, the failure mode changed under monotonic loading; the area surrounding the connectors failed, as in the reference specimen, and both ends of the beams showed uplift. While it remained almost identical when the impact was applied, as shown in Figs. 11 and 12, the only difference was that, under monotonic loading, the crack propagated less, and, for the impacted specimen, buckling in the section appeared due to the increase in ultimate load.

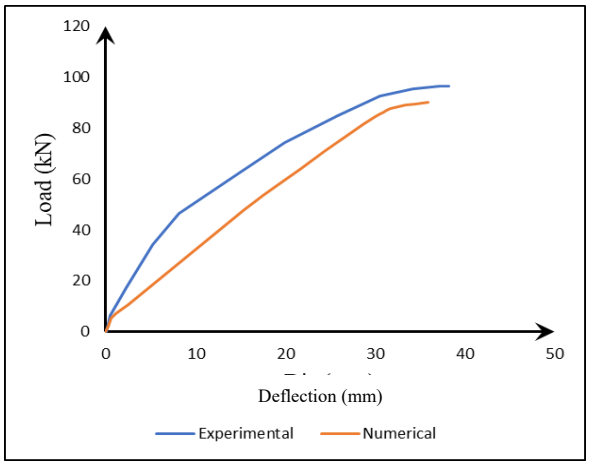


**Figure 7.** Validation of impacted specimens.

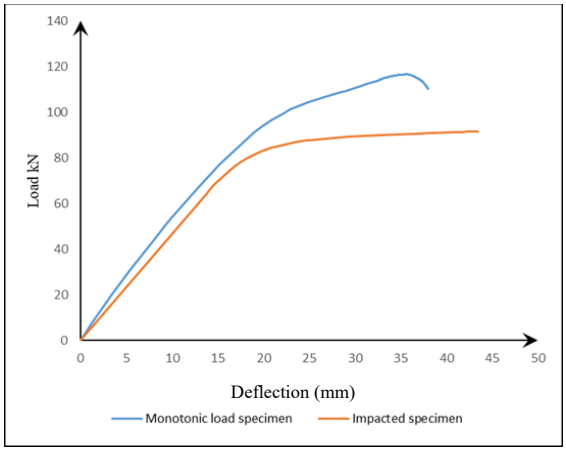


**Figure 8.** Load-displacement curve before and after impact.

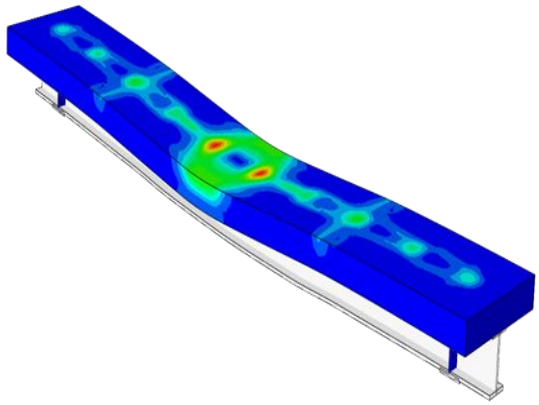

**Figure 9.** Effect of pure monotonic load on the reference specimen.

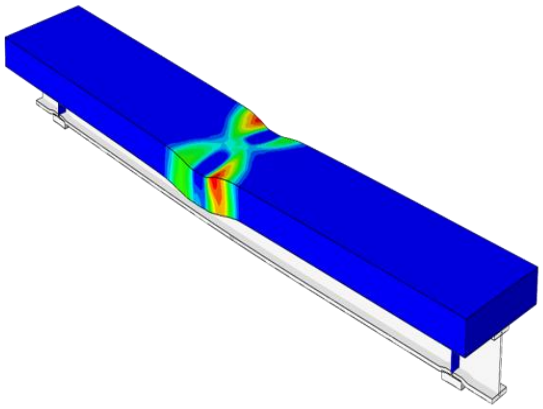

**Figure 10.** Effect of monotonic load after impact on the reference specimen.

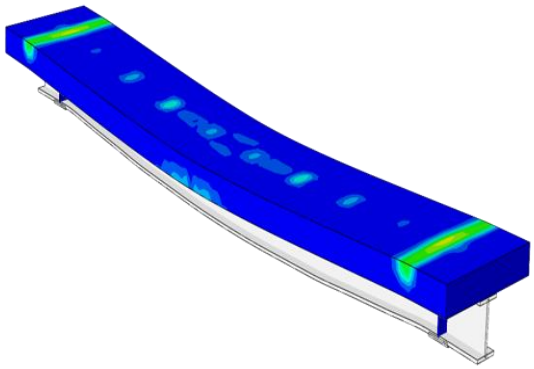

**Figure 11.** Application of monotonic load on 50 MPa concrete.

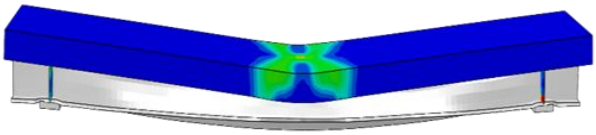

**Figure 12.** Impacted specimen failure mode of the composite beam having 50 MPa concrete slabs.

When 75 and 100 MPa were used, the failure mode changed to tension failure at the bottom face of the concrete slab due to increased concrete strength, with a slight variation in the failure mode at the ends of the beam when 75 MPa was used. As clarified in Figs. 13 and 14.

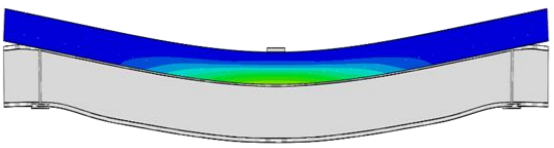

**Figure 13.** Composite beam with a slab of 75 MPa concrete compressive strength subjected to monotonic load.

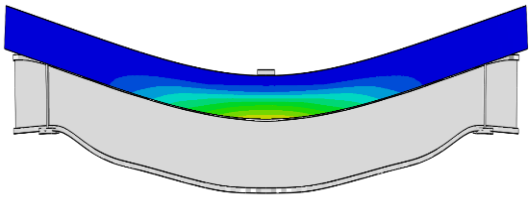

**Figure 14.** Composite beam with a slab of 100 MPa concrete compressive strength subjected to monotonic load.

When the impact was employed, the specimen with 75 MPa exhibited the same failure manner as the 50 MPa and the reference specimen with stiffer failure. When 100 MPa was used, this mode shifted, and the tensile failure occurred near the impact, as in Figs. 15 and 16.

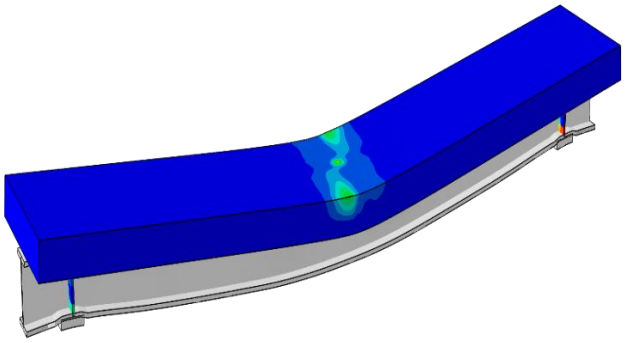

**Figure 15.** Composite beam with a slab of 75 MPa concrete compressive strength subjected to impact load.

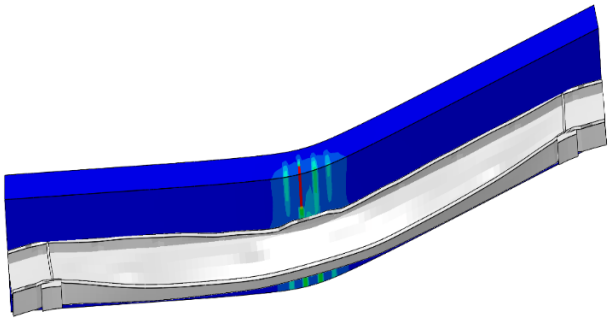

**Figure 16.** Composite beam with a slab of 100 MPa concrete compressive strength subjected to impact load.

In terms of load-deflection behavior, increasing concrete compressive strength increases beam load-bearing capacity for both impacted and non-impacted beams, as well as more brittle failure and a decrease in deflection. For impacted beams, both load capacity and deflection decreased compared with specimens under non-impact loads. For impacted beams, the curve begins linearly, then shifts to nonlinearity as stiffness decreases, before returning to linear behavior due to cracking stabilization and the section's linear response. While the graph

for monotonic load is essentially linear, the rapid reduction in load indicates a sudden failure, as illustrated in Fig. 17, where monotonic refers to specimens subjected to monotonic load only (first group), and impacted refers to specimens subjected to impact load and to monotonic load up to failure after impact.

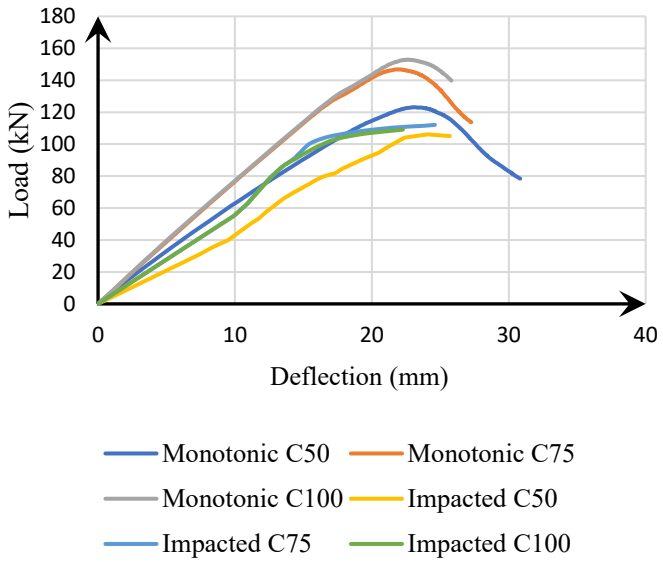


**Figure 17.** Effect of concrete compressive strength and impact loads on load-deflection of the composite beam

*4.1.2. Ductility*

Ductility is a material's or a member's ability to endure deformation beyond the elastic limit while sustaining a reasonable load before total failure. The ductility was calculated using the equation

$$\mu=\frac{\Delta max}{\Delta y} \quad (2)$$

Δmax = max deflection at failure

Δy= deformation at yield

The most practical and reasonable estimate of (Δy) comes from an analogous elastoplastic system with its equivalent elastic stiffness taken as the secant stiffness at 75% of the actual system's ultimate load [33]. For the non-impacted reference specimen and other specimens of concrete compressive strength of (50, 75, and 100) MPa, the ductility was 2.11, 1.852, 1.832, and 1.726, respectively. In contrast, the impacted specimens' ductility values were reduced by 13%, 5%, 3.4%, and 1.4% for the reference specimen and impacts of 50, 75, and 100 MPa, respectively. It can be seen that as the concrete compressive strength increased, the impact damage decreased.

*4.1.3. Stiffness*

The stiffness of composite beams was determined based on the maximum load of the composite beams by taking 45% of the maximum load, dropping it on the (load-deflection) curve, and extracting the deflection value corresponding to this load [34]. The stiffness of composite beams was then determined by dividing the load by the resulting deflection. The stiffness of impacted composite beams was reduced by 27%, 22%, 21%, and 19% compared to the reference specimen at 50, 75, and 100 MPa, respectively. can be seen that as the concrete compressive strength increased, the reduction in stiffness decreased.

### 4.2. Reinforcement Type Effect

*4.2.1. Failure mode and load-displacement behavior*

The mechanism of failure virtually remained the same when the simulated specimens were exposed to monotonic stress, except for specific locations due to the brittle nature of fiber bars, as indicated in Figs. 18 and 19.

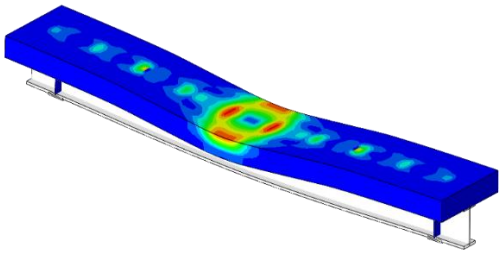

**Figure 18.** Composite beam reinforced by GFRP bars and subjected to monotonic load.

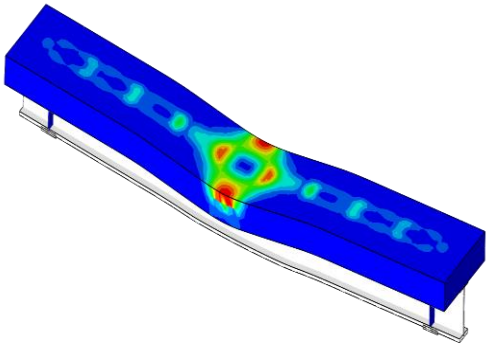

**Figure 19.** Composite beam reinforced by CFRP bars and subjected to monotonic load.

However, when these specimens were subjected to impact, the failure mechanism was altered. When GFRP bars were employed, the failure region extended farther from the impacted area. The slab broke, indicating entire bar failure, as illustrated in Fig. 20. When CFRP bars were utilized, the failure area extended longer than when GFRP bars were used, and the most damaged region was around the impact location, as shown in Fig. 21. These bars outperform GFRP bars in terms of performance.

The load-displacement curves show that the impact significantly affected the beam performance. The maximum load was reduced by 33% and 22% when GFRP and CFRP bars were employed, respectively. However, the steel-reinforced beam maintained good performance at specific load levels

before failing, and the maximum load was reduced by 18.7%, as shown in Fig. 22.

*4.2.2. Ductility*

When different reinforcement bars were used, the ductility of the impacted beams was reduced by 13%, 25%, and 18% for steel, GFRP, and CFRP bars, respectively. When a member is subjected to impact loading, GFRP bars are the most vulnerable due to their brittle nature and poor tensile strength, whereas CFRP bars exhibit excellent yielding and perform better than both GFRP and CFRP bars.

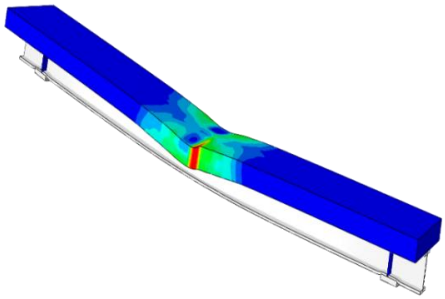

**Figure 20.** Impacted Composite beam reinforced by GFRP bars mode of failure.

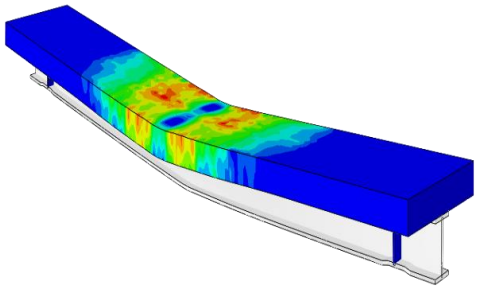

**Figure 21.** Impacted Composite beam reinforced by CFRP bars mode of failure.

*4.2.3. Stiffness*

When the stiffness of impacted composite beams is compared to that of beams subjected to monotonic load only, it can be seen that the beam stiffness decreased by 27%, 40%, and 30% for composite beams reinforced by steel

bars, GFRP bars, and CFRP, respectively. It can be observed that the application of impact loading significantly affects the stiffness of the composite beam, with GFRP bars reducing stiffness by 40%, and steel bars are the best choice for either monotonic or impact loading. Fig. 23 represents the reduction percentages for both ductility and stiffness.

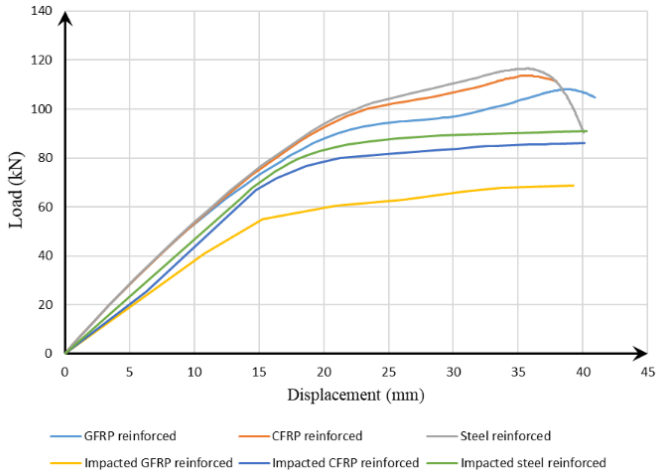


**Figure 22.** Load-displacement behavior of composite beam reinforced by different types of bars

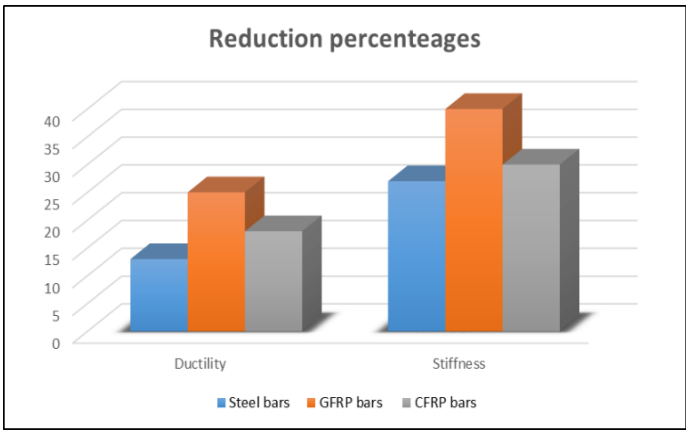


**Figure 23.** Reduction percentages for impacted composite beam stiffness and ductility

Table 1 clarifies the maximum load and deflection for the studied beams.

**Table 1.** Load and deflection values.

| Specimen | Maximum load (kN) | Deflection (mm) | Maximum load after impact (kN) | Deflection after impact (mm) |
|---|---|---|---|---|
| Reference | 116.51 | 35.648 | 90 | 34.378 |
| 50 MPa | 123.166 | 23.329 | 104.396 | 22.396 |
| 75 MPa | 146.839 | 22.945 | 108.123 | 22.231 |
| 100 MPa | 152.88 | 22.673 | 112.092 | 21.832 |
| GFRP reinforced | 108.093 | 38.741 | 72.422 | 26.15 |
| CFRP reinforced | 113.588 | 35.458 | 88.598 | 32.589 |

## 5. Conclusion

In the present work, the behavior of composite beams was numerically investigated using the commercial finite element program ABAQUS 2020. Different concrete compressive strengths were used, and their effects on beam performance were investigated, along with reinforcement bar types. It was concluded that:

The finite element approach is a good method for predicting results that can be experimentally obtained later and for developing an understanding of the numerical results. As the concrete compressive strength increases, the impact effect decreases, and the beam exhibits more brittle behavior; it fails in tension at higher concrete compressive strengths. The ductility was reduced by 25% when the beam was reinforced with GFRP bars and subjected to impact loading. The composite beam stiffness was reduced by almost 40% when GFRP bars were used instead of steel bars; this is due to the brittle behavior and the absence of a yield point in these materials. The CFRP bars reduced the composite beam's stiffness and ductility by 30% and 18%, respectively, due to impact. The steel bars are the best option for composite beam reinforcement, whether monotonic or impact loads are applied; increasing the concrete compressive strength is the best option for strengthening this type of composite beam. Recommendations for future work: Investigate the effect of thermal load on such beams. Investigate the effect of impact load on a composite beam with a prestressed slab.

## Acknowledgments

The authors thank Al-Mustansiriyah University for providing all the administrative and scientific resources necessary to conduct this research.

## Conflict of interest

The authors declare that there are no conflicts of interest regarding the publication of this manuscript.

## Author Contribution Statement

Ayad Hasan Jawad conducted the research and performed the numerical investigation to obtain the results. Hesham A. Numan suggested the article title and structure. Both authors discussed the results and contributed to the final manuscript.

## References

[1] K. Khorramian, S. Maleki, M. Shariati, and N. H. Ramli Sulong, "Behavior of tilted angle shear connectors," *PLOS ONE*, vol. 10, no. 12, Art. no. e0144288, 2015. doi: https://doi.org/10.1371/journal.pone.0144288.

[2] H. Ban, E. L. Tan, and B. Uy, "Strength of multi-span composite beams subjected to combined flexure and torsion," *Journal of Constructional Steel Research*, vol. 113, pp. 1–12, 2015. doi: https://doi.org/10.1016/j.jcsr.2015.05.023

[3] G. K. Abbass and A. H. Aziz, "Structural performance of composite box beams with corroded bottom flange under monotonic and repeated loads," *Journal of Engineering and Sustainable Development*, vol. 27, no. 4, pp. 545–557, 2023. doi: https://doi.org/10.31272/jeasd.27.4.10.

[4] M. M. Nasery, E. Ağcakoca, M. Aydin, and Y. Sümer, "Effects of support type and geometric shape of steel tube on concrete-encased concrete-filled steel tube beam under low velocity impact," *Structures*, vol. 47, pp. 781–799, Jan. 2023. doi: https://doi.org/10.1016/j.istruc.2022.11.075.

[5] T.-L. Chu, Q. H. Pham, and D. X. Quy, "History and applications of concrete steel composite structure," *Ho Chi Minh City Open University Journal of Science - Engineering and Technology*, vol. 12, no. 2, pp. 111–120, 2022. doi: https://doi.org/10.46223/HCMCOUJS.tech.en.12.2.2467.2022.

[6] E. Pelke and K.-E. Kurrer, "On the evolution of steel-concrete composite construction," in *Proc. 5th International Congress on Construction History*, Chicago, IL, USA, 2015, vol. 3, pp. 107–116. [Online]. Available: https://api.semanticscholar.org/CorpusID:116694739

[7] R. S. Nicoletti, A. Rossi, A. S. C. de Souza, and C. H. Martins, "Numerical assessment of effective width in steel-concrete composite box girder bridges with partial interaction," *Engineering Structures*, vol. 239, Art. no. 112333, 2021. doi: https://doi.org/10.1016/j.engstruct.2021.112333.

[8] Li Zongjun, E. (2018). *Impact behavior of hybrid GFRP-concrete beam under low-velocity impact loading.* Thesis, The University of New South Wales, Canberra. https://doi.org/10.26190/unsworks/3398

[9] S. Thondel and J. Studnička, "Behaviour of steel-concrete composite beam with high ribbed deck," *Procedia Engineering*, vol. 40, pp. 457–462, 2012. doi: https://doi.org/10.1016/j.proeng.2012.07.125.

[10] H. A. Numan, "Behavior of composite beam under impact loading," M.Sc. thesis, Civil Engineering Department, Mustansiriyah University, Baghdad, Iraq, 2004

[11] P. Lacki, A. Derlatka, P. Kasza, and S. Gao, "Numerical study of steel–concrete composite beam with composite dowels connectors," *Computers & Structures*, vol. 255, Art. no. 106618, 2021. doi: https://doi.org/10.1016/j.compstruc.2021.106618.

[12] N. Loqman, N. A. Safiee, N. A. Bakar, and N. A. M. Nasir, "Structural behavior of steel-concrete composite beam using bolted shear connectors: A review," *MATEC Web of Conferences*, vol. 203, Art. no. 06010, 2018. doi: https://doi.org/10.1051/matecconf/201820306010.

~~[12] G. Long, R. Zhou, H. Ma, G. Xin, S. Emadi, and X. Shi, "Experimental and numerical study on UHPC–RC decks within hogging moment region," *Applied Sciences*, vol. 12, no. 22, Art. no. 11446, 2022. doi: https://doi.org/10.3390/app122211446.~~

[13] H. A. Numan, "Linear analysis of continuous composite concrete-steel beam with partial connection," *Journal of Engineering and Sustainable Development*, vol. 13, no. 2, pp. 1–19, Jun. 2009. [Online]. Available: https://jeasd.uomustansiriyah.edu.iq/index.php/jeasd/article/view/1553

[14] T. A. Mohammed and S. Abebe, "Numerical investigation of steel-concrete composite (SCC) beam subjected to combined blast-impact loading," *Heliyon*, vol. 8, no. 9, Art. no. e10672, 2022. doi: https://doi.org/10.1016/j.heliyon.2022.e10672.

[15 T. P. J. Leskinen, "Comparison of static and dynamic biomechanical models," *Ergonomics*, vol. 28, no. 1, pp. 285–291, 1985, doi: https://doi.org/10.1080/00140138508963135

[16] N. Razali, M. T. H. Sultan, F. Mustapha, N. Yidris, and M. R. Ishak, "Impact damage on composite structures: A review," *The International Journal of Engineering and Science*, vol. 3, no. 7, pp. 8–20, 2014. [Online]. Available: https://api.semanticscholar.org/CorpusID:139000285.

[17] J. Fan, J. Nie, Q. Li, and H. Wang, "Long-term behavior of composite beams under positive and negative bending. I: Experimental study," *Journal of Structural Engineering*, vol. 136, no. 7, pp. 849–857, Jul. 2010. doi: https://doi.org/10.1061/(ASCE)ST.1943-541X.0000175.

[18] W. G. Machado, F. de A. Neves, and J. B. M. de Sousa, "Parametric modal dynamic analysis of steel-concrete composite beams with deformable shear connection," *Latin American Journal of Solids and Structures*, vol. 14, no. 2, pp. 335–356, 2017. doi: https://doi.org/10.1590/1679-78252981.

[19] G. Zhao and A. Li, "Numerical study of a bonded steel and concrete composite beam," *Computers & Structures*, vol. 86, no. 19–20, pp. 1830–1838, Oct. 2008. doi: https://doi.org/10.1016/j.compstruc.2008.04.002.

[20] R. Shamass and K. A. Cashell, "Behaviour of composite beams made using high strength steel," *Structures*, vol. 12, pp. 88–101, Nov. 2017. doi: https://doi.org/10.1016/j.istruc.2017.08.005.

[21] J. C. Xiao, J. F. Liu, C. Bai, J. Y. Mao, and K. J. Ma, "Dynamic behavior of composite beams under impact load," *Key Engineering Materials*, vols. 400–402, pp. 783–787, 2008. doi: https://doi.org/10.4028/www.scientific.net/KEM.400-402.783.

[22] M. J. Hamood, S. M. Sabih, and M. G. Ghaddar, "Numerical simulation of composite beam subjected to harmonic force vibration," *International Review of Civil Engineering*, vol. 12, no. 2, pp. 93–100, Mar. 2021. doi: https://doi.org/10.15866/irece.v12i2.18590.

[23] Y.-F. Yang, Z.-C. Zhang, and F. Fu, "Experimental and numerical study on square RACFST members under lateral impact loading," *Journal of Constructional Steel Research*, vol. 111, pp. 43–56, 2015. doi: https://doi.org/10.1016/j.jcsr.2015.04.004

[24] A. A. Jaafer and S. L. Kareem, "Behavior of curved steel-concrete composite beams under monotonic load," *International Journal of Mathematical, Engineering and Management Sciences*, vol. 5, no. 6, pp. 1210–1233, 2020. doi: https://doi.org/10.33889/IJMEMS.2020.5.6.091.

[25] R. E. S. Ismail, A. S. Fahmy, and N. M. Tawfik, "Ultimate behavior of composite castellated beams under vertical loads," *International Journal of Computer Applications*, vol. 108, no. 5, pp. 40–46, Dec. 2014. doi: https://doi.org/10.5120/18911-0214.

[26] J. Liu, F. X. Ding, X. M. Liu, Z. W. Yu, Z. Tan, and J. W. Huang, "Flexural capacity of steel-concrete composite beams under hogging moment," *Advances in Civil Engineering*, vol. 2019, Art. no. 3453274, 2019. doi: https://doi.org/10.1155/2019/3453274.

[27] C. A. Neagoe, L. Gil, and M. A. Pérez, "Experimental study of GFRP-concrete hybrid beams with low degree of shear connection," *Construction and Building Materials*, vol. 101, pp. 141–151, Dec. 2015. doi: https://doi.org/10.1016/j.conbuildmat.2015.10.024.

[28] A. A. Allawi and S. I. Ali, "Flexural behavior of composite GFRP pultruded I-section beams under static and impact loading," *Civil Engineering Journal*, vol. 6, no. 11, pp. 2143–2158, Nov. 2020. doi: https://doi.org/10.28991/cej-2020-03091608.

[29] M. N. S. Hadi and J. S. Yuan, "Experimental investigation of composite beams reinforced with GFRP I-beam and steel bars," *Construction and Building Materials*, vol. 144, pp. 462–474, Jul. 2017. doi: https://doi.org/10.1016/j.conbuildmat.2017.03.217.

[30] A. K. M. Anwarul Islam, "Effective methods of using CFRP bars in shear strengthening of concrete girders," *Engineering Structures*, vol. 31, no. 3, pp. 709–714, Mar. 2009. doi: https://doi.org/10.1016/j.engstruct.2008.11.016.

[31] ABAQUS, "ABAQUS 6.14 Analysis User's Guide," *ABAQUS 6.14 Anal. User's Guid.*, vol. IV, pp. 1–1128, 2014, [Online]. Available: http://130.149.89.49:2080/v6.14/books/usb/default.htm.

[32] M. Goldston, A. Remennikov, and M. N. Sheikh, "Experimental investigation of the behaviour of concrete beams reinforced with GFRP bars under static and impact loading," *Engineering Structures*, vol. 113, pp. 220–232, Apr. 2016. doi: https://doi.org/10.1016/j.engstruct.2016.01.044.

[33] R. Park, "Ductility evaluation from laboratory and analytical testing," in *Proc. 9th World Conference on Earthquake Engineering*, Tokyo-Kyoto, Japan, Aug. 2–9, 1988, vol. 8, pp. 605–616. [Online]. Available: https://www.iitk.ac.in/nicee/wcee/article/9_vol8_605.pdf

[35] S. R. Al-Jawary, "Behavior of reinforced concrete beams strengthened with near-surface mounted carbon fiber reinforced polymer," M.Sc. thesis, Civil Engineering Department, University of Mosul, Mosul, Iraq, 2010.